Available online at www.sciencedirect.com

ScienceDirect

Catalysis Today 117 (2006) 242–247

CATALYSIS TODAY

www.elsevier.com/locate/cattod

Preparation of palladium oxide nanoparticles-encapsulating porous oxide catalysts for oxidation utilizing a silsesquioxane ligand

Kenji Wada *, Kousuke Yano, Teruyuki Kondo, Take-aki Mitsudo *

Department of Energy and Hydrocarbon Chemistry, Graduate School of Engineering, Kyoto University, Nishikyo-ku, Kyoto 615-8510, Japan

Abstract

The controlled calcination of Pd complexes bearing a silsesquioxane-amine ligand $(c\text{-}C_5H_9)_7Si_7O_{10}\{OSi(Me_2)CH_2CH_2CH_2NH_2\}$ (**1**), at 823 K in air stream for 4 h afforded porous silicas of high surface areas and uniformly controlled micropores of ca. 0.6 nm diameter encapsulating monodispersed palladium oxide nanoparticles. The calcination after the impregnation of palladium complexes bearing **1** onto titanium oxide afforded oxides with both meso- and micropores. These catalysts showed excellent catalytic activities towards the aerobic oxidation of benzyl alcohol, especially even in water (benzaldehyde yield up to 87% in air at 353 K for 24 h with 0.10 mol% Pd).

Keywords: Catalysts; Oxidation; Palladium; Porous materials; Silsesquioxane

1. Introduction

The selective oxidation of small organic molecules, such as alcohols with air is of significance from both the academic and industrial viewpoints, and a number of heterogeneous catalysts have been developed for several decades [1–3]. Recently, excellent catalytic activities of palladium cations or clusters supported on TiO_2, hydrotalcite, hydroxyapatite, polymer, and active carbon for the oxidation of benzylic and/or allylic alcohols to the corresponding aldehydes in organic solvents have been reported [4–19]. While some of these catalysts were found to show some activities even in water [16,19], the development of novel types of catalyst with higher efficiency for reactions in water, an economical, safe, and environmentally benign solvent, is greatly desired [20].

On the other hand, polyhedral oligosilsesquioxanes have attracted attention mainly from the viewpoint as building blocks of novel inorganic–organic hybrid materials or soluble model compounds of siliceous solid catalysts [21–30]. Several ligands bearing a silsesquioxane moiety have been also synthesized and utilized for the preparation of transition metal complexes [31], or nanoclusters [32–36]. Silsesquioxanes, especially metal-containing ones, have also been utilized as excellent precursors of heterogeneous catalysts [25,37–47]. Note that the present authors have found for the first time that porous oxides with large surface areas and uniformly controlled micropores can be prepared by the controlled calcination of metal-containing oligosilsesquioxanes [37–41].

Against this background, one can expect the preparation of microporous silica including small particles of a transition metal species by the controlled calcination of transition metal complexes bearing silsesquioxane ligands.

Herein, we report the preparation of novel silica catalysts with controlled micropores encapsulating monodispersed palladium oxide nanoparticles by the calcination of palladium complexes bearing a silsesquioxane-amine ligand **1**. Furthermore, multi-component oxide catalysts with bimodal pore structures encapsulating nanoparticles of palladium oxide (1.5–3.0 nm) were prepared by combination with titanium oxide followed by the calcination. The excellent activities and selectivity of these catalysts, especially titanium oxide-supported ones, towards the aerobic oxidation of benzyl alcohol in water media are presented.

2. Experimental

2.1. Materials or methods

All manipulations for the preparation of silsesquioxane ligands and complexes were performed under an argon

---

* Corresponding authors. Tel.: +81 75 383 2511; fax: +81 75 383 2510.
E-mail address: wadaken@scl.kyoto-u.ac.jp (K. Wada).

0920-5861/$ – see front matter © 2006 Elsevier B.V. All rights reserved.
doi:10.1016/j.cattod.2006.05.024

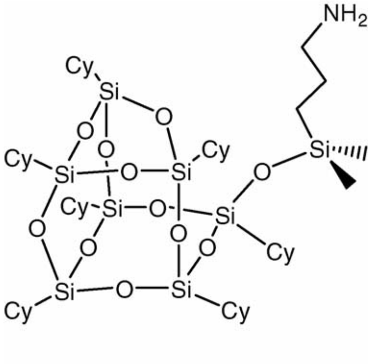

1 (Cy = c-C_5H_9)

Scheme 1.

atmosphere using standard Schlenk techniques. All solvents were distilled under argon over appropriate drying reagents [48]. Silsesquioxane trisilanol ((c-$C_5H_9)_7Si_7O_9(OH)_3$, Aldrich), aminopropyldimethylethoxysilane (Aldrich), and $Pd(OAc)_2$ (Nacarai Tesque) were obtained commercially and used without further purification. Titanium oxide (Nihon Aerosil P-25) was used after the evacuation at 413 K for 16 h. The preparation method of a silsesquioxame-amine ligand **1** has been described elsewhere [49] (Scheme 1).

2.2. Physical and analytical measurements

IR spectra were recorded using a Nicolet Impact 410 FT-IR spectrometer. The oxide catalysts were analyzed by nitrogen gas adsorption, X-ray diffraction (XRD), FTIR, X-ray photoelectron spectra (XPS), TEM, SEM, and so on. Nitrogen adsorption/desorption isotherms were obtained with a Quantachrome Autosorb 1-MP, a computer-controlled automatic gas sorption system. Samples were degassed at 573 K for 2 h just before the measurements. XRD study was performed using a Shimadzu XD-D1 with $K\alpha_{1,2}$-emission of copper in the range $5^\circ < 2\theta < 70^\circ$. XPS of the catalysts were acquired using an ULVAC-PHI 5500MT system equipped with a hemispherical energy analyzer. Samples were mounted on indium foil and then transferred to an XPS analyzer chamber. The residual gas pressure in the chamber during data acquisition was less than 1×10^{-8} Torr ($1\ \text{Torr} = 133.3\ \text{N m}^{-2}$). The spectra were measured at room temperature using Mg $K\alpha_{1,2}$ radiation (15 kV, 400 W). The electron take-off angle was set at 45°. Binding energies were referenced to C1s level of residual graphitic carbon [50]. Sputtering was performed by Xe^+ ion beam generated at 3.0 kV. The TEM observation was performed using a Hitachi H-9000 transmission electron microscope (300 kV). The apparent shape and size of the oxide particles were observed using a Hitachi S-2500 CX scanning electron microscope (SEM). The oxidation products were analyzed by GC-MS (Shimadzu QP 5000, CBP10-S25-050 capillary column, i.d. 0.33 mm, length 25 m, o.d. 0.43 mm at 323–473 K) and gas chromatography (Shimadzu GC14BPF, CBP10-S25-050 capillary column, i.d. 0.33 mm, length 25 m, o.d. 0.43 mm at 323–473 K). The ICP atomic emission spectroscopic analysis was performed by using a Seiko Instruments SPS 3100 analyzer.

2.3. Preparation of Pd^{2+}-*1*(2)-823

Palladium(II) acetate (0.20 mmol) and **1** (0.40 mmol) were stirred in toluene ($20\ \text{cm}^3$) overnight at room temperature under argon to afford a clear yellow solution including Pd complexes. After evaporation of the solvent, 0.50 g of the resulting yellow powder was calcined in a stream of dried, CO_2-free air ($W/F = 2.0\ \text{g h mol}^{-1}$) by using a fixed-bed flow type quartz reactor (i.d. 8.0 mm) under atmospheric pressure. Temperature was raised by $10\ \text{K min}^{-1}$ from 423 to 823 K, and held for 4 h. The calcined catalyst was carefully recovered with minimal contact with air and moisture, and stored under an argon atmosphere. TEM and SEM analyses showed that Pd^{2+}-**1**(2)-823 consists of large cube-like particles (ca. 10 μm × 10 μm × 10 μm). The XRD pattern shows no distinct peaks for a crystalline silica or palladium species, indicating its amorphous nature.

2.4. Preparation of TiO_2-supported oxide catalysts

A clear, yellow toluene solution ($20\ \text{cm}^3$) including palladium complexes (Pd 0.20 mmol, **1** 0.40 mmol) was added to titanium oxide (0.50 g, vacuum-dried at 413 K for 16 h) and stirred vigorously at room temperature for 24 h. For Pd^{2+}-**1**(5)-TiO_2-823, the amount of $Pd(OAc)_2$ was reduced to 0.080 mmol. After removal of the volatiles, the resulting solid was calcined in air ($W/F = 2.0\ \text{g h mol}^{-1}$) at 823 K for 4 h (see above).

2.5. Typical procedure for the aerobic oxidation of benzyl alcohol

Under air (open), a prescribed amount of the catalyst (0.10 or 0.40 mol% as Pd) and a toluene solution of benzyl alcohol ($3.0\ \text{cm}^3$) were added to a $10\ \text{cm}^3$ Schlenk tube equipped with a Teflon-coated stirring bar. The mixture was stirred at 353 K for 24 h with the use of a hot magnetic stirrer equipped with stainless steel cooling blocks. The products were analyzed by GC (internal standard: naphthalene) and GC-MS.

3. Results and discussion

3.1. Preparation of microporous siliceous oxides from silsesquioxane–Pd complexes

Treatment of palladium acetate with two equivalents of a silsesquioxane ligand **1** in toluene for 24 h at room temperature afforded a clear yellow solution. After evaporation of the solvent, yellow powder was obtained. Although complete separation and identification of the products have not been achieved yet, shift of the IR bands of the C=O stretching of acetate ligands to higher wavenumbers by $5\ \text{cm}^{-1}$ suggests the formation of a mixture of complexes including $Pd(OAc)_2(\text{ligand})_2$—type one [51].

Table 1
BET surface areas of the catalysts and titanium oxide

Catalyst	Surface area ($m^2\ g^{-1}$)
Pd^{2+}-**1**(2)-823	433
Pd^{2+}-**1**(2)-TiO_2-823	188
Pd^{2+}-**1**(5)-TiO_2-823	279
TiO_2-823	47

The controlled calcination of the mixture of palladium complexes bearing **1** at 823 K in a stream of air for 4 h produced amorphous microporous siliceous oxides, hereafter designated as Pd^{2+}-**1**(2)-823 (numbers in parentheses show the molar ratio of **1** to $Pd(OAc)_2$ in the starting mixtures, and the suffix 823 stands for the calcination temperature in K). Table 1 shows the BET surface area of Pd^{2+}-**1**(2)-823. This oxide shows the type-I nitrogen adsorption/desorption isotherm characteristic of truly microporous materials (Fig. 1) [52]. Pore size distribution estimated from the nitrogen adsorption isotherms by the Saito–Foley method [53] shows a peak at around 0.6 nm. Its pore texture is very close to that of HZSM-5 zeolite.

Fig. 2 shows a TEM photograph of palladium oxide nanoparticles of Pd^{2+}-**1**(2)-823, which revealed the formation of nanoparticles of the palladium species with a narrow size distribution (5–7 nm) encapsulated in microporous silica. Remarkably, almost all of the palladium nanoparticles were covered with a silica layer and were not exposed to the outer surface.

3.2. Preparation of oxides with bimodal pore structure from TiO_2-supported silsesquioxane–Pd complexes

Preparation of the catalysts having both micro- and mesopores by the combination with titanium oxides was examined. The impregnation of vacuum-dried titanium oxide (P-25) with a prescribed amount of a mixture of palladium complexes bearing **1** followed by calcination at 823 K for 4 h in a stream of air yielded three-component porous oxides (further designated as Pd^{2+}-**1**(5)-TiO_2-823). The BET surface areas of the calcined oxides and titanium oxide are presented in Table 1. Remarkably, the BET surface areas of calcined supported catalysts were significantly higher than that of the parent titanium oxide. Fig. 3 shows nitrogen adsorption/desorption isotherms of Pd^{2+}-**1**(5)-TiO_2-823, Pd^{2+}-**1**(2)-TiO_2-823, and titanium oxide. The Pd^{2+}-**1**(5)-TiO_2-823 catalyst adsorbed a considerable amount of nitrogen at very low relative pressure compared with titanium oxide, implying the formation of a microporous structure. Analysis by the Saito–Foley method also indicates the uniformity of pore size (ca. 0.6 nm). The supported catalyst has ink bottle-shaped mesopores interconnected by micropores, as indicated by the presence of a wedge-shaped histerisis (type-H2) [52] in its desorption isotherm. The isotherms of as Pd^{2+}-**1**(2)-TiO_2-823 also show the presence of ink bottle-shaped mesopores. Peaks attributable to the crystalline Pd species cannot be confirmed by XRD analysis.

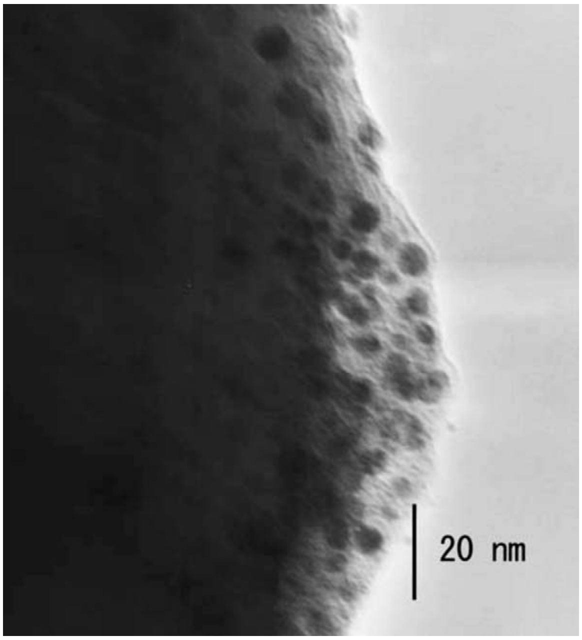

Fig. 2. TEM photograph of Pd^{2+}-**1**(2)-823.

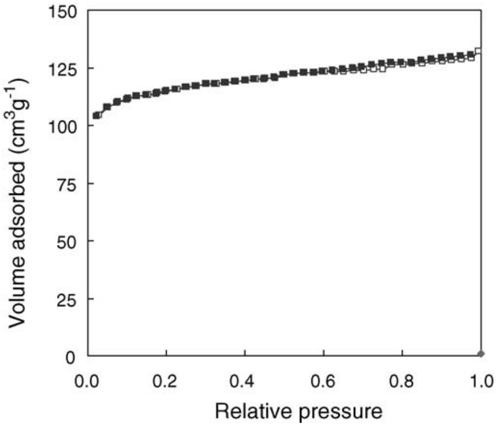

Fig. 1. Nitrogen adsorption/desorption isotherms of Pd^{2+}-**1**(2)-823. Open and filled marks stand for adsorption and desorption data, respectively.

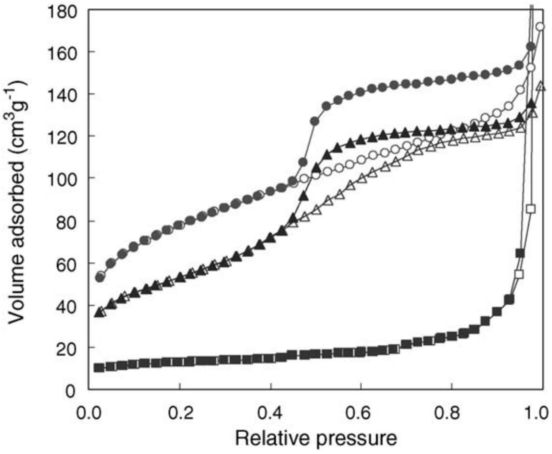

Fig. 3. Nitrogen adsorption/desorption isotherms of Pd^{2+}-**1**(5)-TiO_2-823 (circles), Pd^{2+}-**1**(2)-TiO_2-823 (triangles), and TiO_2-823 (squares). Open and filled marks stand for adsorption and desorption data, respectively.

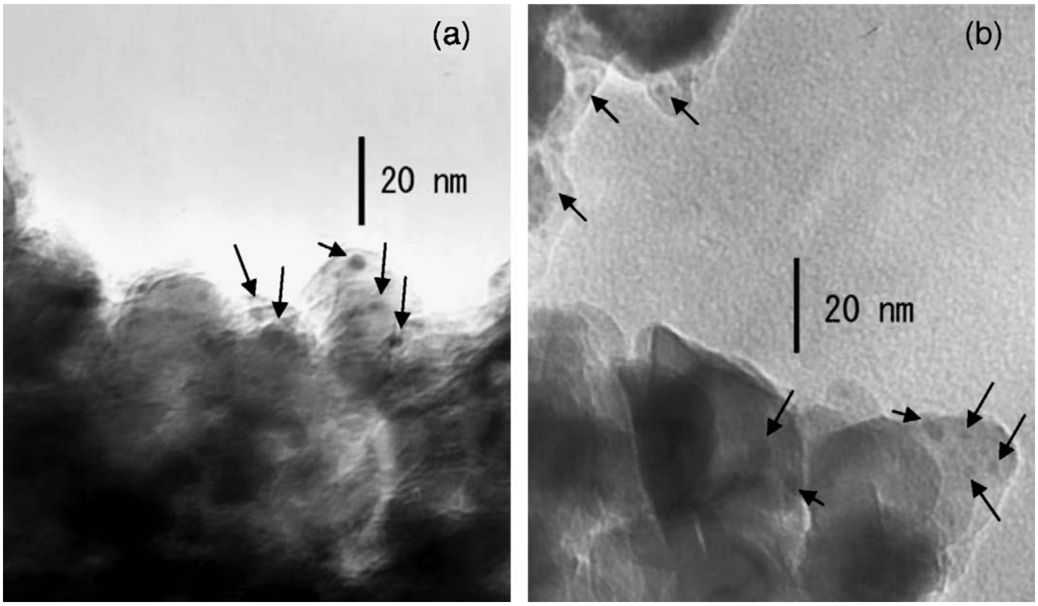

Fig. 4. TEM Photographs of Pd^{2+}-**1**(5)-TiO_2-823 (a) before and (b) after the catalytic run (run 8 in Table 3).

Fig. 4a shows a TEM photograph of fresh Pd^{2+}-**1**(5)-TiO_2-823 catalyst. The formation of an ultrathin layer of amorphous silica (2–5 nm thickness) over the surface of titanium oxide crystalline particles is recognized. Palladium oxide nanoparticles of ca. 1.5–3.0 nm in diameter were found to be encapsulated in the silica layer.

The results of XPS analysis of Pd^{2+}-**1**(5)-TiO_2-823 are consistent with the coverage of the palladium species and titanium oxide particles with an ultrathin silica layer. As shown in Table 2, the surface atomic ratios of Si/Ti and Si/Pd were very high, but both markedly decreased by the sputtering. The Pd $3d_{5/2}$ peaks appeared at around 336.2 eV, indicating the presence of Pd^{2+} species [50]. After the catalytic reaction, the outermost surface of the palladium oxide nanoparticles was reduced to Pd^0 (Pd $3d_{5/2}$ at 335.0 eV). Fig. 5 shows the proposed structure of the titanium oxide-supported catalysts based on the observation described above.

Note that the oxide prepared using silsesquioxanes without amino groups, such as $(c\text{-}C_5H_9)_7Si_7O_9(OSiMe_3)(OH)_2$, in place of the silsesquioxane amine ligand **1** showed significantly low surface Si/Ti ratios, indicating that the silica layer did not fully cover the surface of TiO_2 support. This implies that coordinating groups of the silsesquioxane ligands play a significant role not only for the formation of nanoparticles of transition metal species but also for the formation of well-dispersed thin silica layer, probably because of the significant interaction of the ligands with the TiO_2 surface.

3.3. Catalytic activity of the porous silica-titanium oxide catalysts encapsulating PdO nanoparticles

The catalytic activities of thus-prepared porous oxides towards the aerobic oxidation of benzyl alcohol typically in air at 353 K for 24 h (Eq. (1)) were examined in toluene or water. Table 3 shows the conversions of benzyl alcohol and yields of benzaldehyde. In the case with titanium oxide-supported catalysts a major byproduct was dibenzyl ether, probably formed at the surface acidic sites of the catalysts. Only the reactions for longer period than 24 h yielded a trace amount of benzoic acid as one of byproducts. Although the activity of Pd^{2+}-**1**(2)-823 was low in toluene, a higher yield of benzaldehyde was recorded in water (runs 1–2). The titanium oxide-supported catalysts exhibited excellent activities. Our preliminary investigation using several oxide supports, silica, aluminum oxide, titanium oxide, shows that titanium oxide is the most suitable support and the most suitable calcination temperature is about 823 K, like

Table 2
XPS analysis of the Pd^{2+}-**1**(5)- TiO_2-823 catalyst[a]

Remarks	Sputtering (min)	C (%)	Si (%)	Ti (%)	Pd (%)	O (%)	Si/Ti ratio	Si/Pd ratio	Pd3$d_{5/2}$ (eV)
Before the reaction	0	4.24	24.46	4.47	0.19	66.47	5.47	129	336.2
	1	1.31	21.02	10.82	0.23	66.37	1.94	91	336.2
	2	0.71	18.44	13.63	0.23	66.66	1.35	80	336.5
	3	0.68	16.82	15.73	0.24	66.12	1.07	70	336.4
	5	0.69	15.13	17.56	0.25	65.89	0.86	61	336.7
After the reaction[b]	0	12.93	20.03	5.38	0.16	61.44	3.72	125	335.0

[a] Surface concentrations are shown as atomic %.

[b] After run 8 in Table 3.

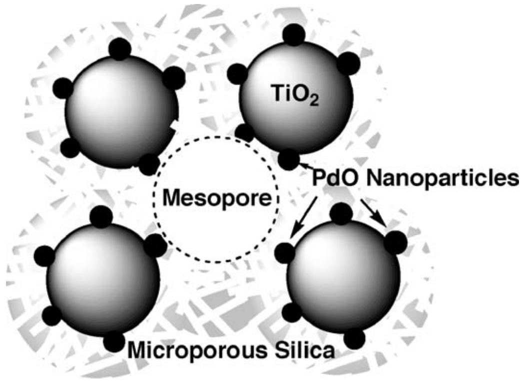

Fig. 5. Supposed schematic structure of the titanium oxide-supported catalysts.

other oxide catalysts from silsesquioxanes [37–47]. For these catalysts, as shown in Table 3, the yields of benzaldehyde in water were not decreased in comparison with those in toluene. Note that the formation of the byproduct, dibenzyl ether, was significantly suppressed in water. These catalysts can be reused without loss of their activities, as shown in run 5. Among the catalysts examined, Pd^{2+}-**1**(5)-TiO_2-823 selectively gave benzaldehyde in the highest yield of 87% in water (run 8). In toluene this catalyst yielded much amount of dibenzyl ether. The reaction with a significantly larger amount of neat benzyl alcohol yielded 5.07 mmol (18%) of benzaldehyde together with 0.71 mmol (5.2%) of dibenzyl ether (run 6), resulting in the production of only slightly higher amount of benzaldehyde than the case of the reaction in water (4.35 mmol, run 8). Note that there were no significant changes in the surface Si/Pd ratios of the catalysts before and after the reactions by the XPS analysis (see Table 2). The comparison of TEM photographs of Pd^{2+}-**1**(5)-TiO_2-823 before (Fig. 4a) and after (Fig. 4b) the catalytic run (run 8 in Table 3) shows that there are no significant changes in the size and dispersion of palladium oxide nanoparticles during the catalytic run. The ICP atomic emission spectroscopy clearly indicates the absence of leaching of Pd species into the reaction mixture.

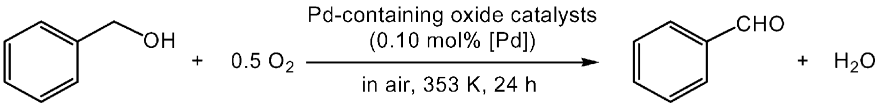

(1)

Table 3
Catalytic activities of palladium oxide-containing porous oxide catalysts[a]

Run	Catalyst (mol%[Pd])	Solvent	Conversion (%)[b]	Yield (%)[b]
1	Pd^{2+}-**1**(2)-823 (0.40)	Toluene	6	6
2	Pd^{2+}-**1**(2)-823 (0.40)	Water	36	35
3	Pd^{2+}-**1**(2)-TiO_2-823(0.10)	Toluene	100	61
4	Pd^{2+}-**1**(2)-TiO_2-823(0.10)	Water	87	61
5	Pd^{2+}-**1**(2)-TiO_2-823 (0.09)[c]	Water	94	59
6	Pd^{2+}-**1**(5)-TiO_2-823(0.10)	–[d]	–[e]	18
7	Pd^{2+}-**1**(5)-TiO_2-823(0.10)	Toluene	87	38
8	Pd^{2+}-**1**(5)-TiO_2-823(0.10)	Water	87	87
9	Pd^{2+}-TiO_2-823(0.10)	Toluene	97	67
10	Pd^{2+}-TiO_2-823(0.10)	Water	34	20

[a] Reaction conditions: benzyl alcohol 5.0 mmol, solvent 3.0 cm^3, 353 K, under air, 24 h.
[b] Determined by GLC.
[c] Reused catalyst.
[d] Benzyl alcohol 27.6 mmol was used without a solvent.
[e] Not determined.

In the case of using the Pd^{2+}-TiO_2-823 catalyst prepared without **1**, the yields of benzaldehyde significantly decreased by changing the solvent from toluene to water (run 10), implying the crucial effect of the ultrathin microporous silica layer derived from **1** on the catalyst surface on the catalytic activity in water media. As one possible reason for their excellent activities in water, the presence of both nano-sized highly hydrophilic silica domains and a titanium oxide surface with higher alcohol affinity [54–56] would promote the access of both reactant and oxidant towards the catalytically active palladium species. In addition, the suppression of the dibenzyl ether formation should be another reason. Note that the TEM observation shows the formation of large PdO particles (>5 nm) on the surface of the Pd^{2+}-TiO_2-823 catalyst, indicating that the use of **1** greatly suppress the growth of PdO particles during the calcination.

While the oxidation of a more bulky alcohol, 2-naphthylmethanol, in the presence of Pd^{2+}-TiO_2-823 gave the corresponding aldehyde (yield 12%, in toluene), the reaction did not proceed with Pd^{2+}-**1**(5)-TiO_2-823 under the identical conditions, suggesting the size selectivity of the catalysts due to the microporous thin silica layer on its surface. Further study on the size selectivity of thin microporous silica layer is now proceeding.

4. Conclusion

The present study shows the preparation of silicas with uniformly controlled micropores encapsulating monodispersed palladium oxide nanoparticles by the controlled calcination of palladium complexes bearing a silsesquioxane-amine ligand **1**. The calcination after the impregnation of titanium oxide (P-25) with a palladium species including **1** afforded oxides having both uniformly controlled micropores and ink bottle-type mesopores. These catalysts included palladium oxide nanoparticles of 1.5–3.0 nm diameter, which are located on the surface of titanium oxide crystalline particles and covered by an ultrathin microporous silica layer. These titanium oxide-supported catalysts showed excellent catalytic activities towards the aerobic oxidation of benzyl alcohol in water. The ultrathin microporous silica layer is responsible for the enhancement of the catalytic activity in water, the suppression of the growth of PdO particles during the calcination, and the induction of the size selectivity of the catalysts.

As shown here, transition metal complexes bearing silsesquioxane ligands are found to be excellent precursors of oxide catalysts encapsulating highly dispersed nanoparticles of transition metal species with well-defined, characteristic pore structures. Attempts to use these materials as the catalysts for various organic transformations in the water media and as the automobile catalysts are now proceeding.

Acknowledgements

This work was supported by a Grant-in Aid for Scientific Research (No. 16560676) and Grant-in-Aids for 21st century COE program, COE for a United Approach to New Materials Science, from the Japan Society of the Promotion of Science and the Ministry of Education, Sports, Culture, Science, and Technology, Japan. K.W. acknowledges financial support from the Kurita Water and Environment Foundation. We thank Prof. Z. Ogumi and Dr. Y. Iriyama of Kyoto University for their kind help in the TEM observation.

References

[1] R.A. Sheldon, J.K. Kochi, Metal-Catalyzed Oxidations of Organic Compounds, Academic Press, New York, USA, 1981.

[2] M. Hudlicky, Oxidations in Organic Chemistry, ACS Monograph Series, American Chemical Society, Washington, DC, USA, 1990.

[3] I.W.C.E. Arends, R.A. Sheldon, Appl. Catal. A Gen. 212 (2001) 175.

[4] T. Mallat, A. Baiker, Chem. Rev. 104 (2004) 3037.

[5] R.A. Sheldon, M. Wallau, I.W.C.A. Arends, U. Schuchardt, Acc. Chem. Res. 31 (1998) 485.

[6] T. Nishimura, N. Kakiuchi, M. Inoue, S. Uemura, Chem. Commun. (2000) 1245.

[7] N. Kakiuchi, T. Nishimura, M. Inoue, S. Uemura, Bull. Chem. Soc. Jpn. 74 (2001) 165.

[8] N. Kakiuchi, Y. Maeda, T. Nishimura, S. Uemura, J. Org. Chem. 66 (2001) 6620.

[9] K. Kaneda, M. Fujii, K. Morioka, J. Org. Chem. 61 (1996) 4502.

[10] K. Kaneda, Y. Fujie, K. Ebitani, Tetrahedron Lett. 38 (1997) 9023.

[11] K. Ebitani, Y. Fujie, K. Kaneda, Langmuir 15 (1999) 3557.

[12] K. Ebitani, K.M. Choi, T. Mizugaki, K. Kaneda, Langmuir 18 (2002) 1849.

[13] K. Mori, K. Yamaguchi, T. Hara, T. Mizugaki, K. Ebitani, K. Kaneda, J. Am. Chem. Soc. 124 (2002) 11572.

[14] K.M. Choi, T. Akita, T. Mizugaki, K. Ebitani, K. Kaneda, New J. Chem. 27 (2003) 324.

[15] K.M. Choi, T. Mizugaki, K. Ebitani, K. Kaneda, Chem. Lett. 32 (2003) 180.

[16] K. Mori, T. Hara, T. Mizugaki, K. Ebitani, K. Kaneda, J. Am. Chem. Soc. 126 (2004) 10657.

[17] T. Mallat, A. Baiker, Catal. Today 19 (1994) 247.

[18] L.F. Liotta, A.M. Venezia, G. Deganello, A. Longo, A. Martorana, Z. Schay, L. Guczi, Catal. Today 66 (2001) 271.

[19] Y. Uozumi, R. Nakao, Angew. Chem. 115 (2003) 204;
Y. Uozumi, R. Nakao, Angew. Chem. Int. Ed. 42 (2003) 194.

[20] C.-J. Li, T.-H. Chan (Eds.), Organic Reactions in Aqueous Media, Wiley, New York, USA, 1997.

[21] R.H. Baney, M. Ito, A. Sakakibara, T. Suzuki, Chem. Rev. 95 (1995) 1409.

[22] F.J. Feher, T.A. Budzichowski, Polyhedron 14 (1995) 3239.

[23] R. Murugavel, A. Voigt, M.G. Walawalker, H.W. Roesky, Chem. Rev. 96 (1996) 2205.

[24] P.G. Harrison, J. Organomet. Chem. 542 (1997) 141.

[25] H.C.L. Abbenhuis, Chem. Eur. J. 6 (2000) 25.

[26] T. Mitsudo, K. Wada, Shokubai 42 (2000) 282.

[27] V. Lorenz, A. Fischer, S. Giessmann, J.W. Gilje, Y. Gun'ko, K. Yacob, F.T. Edelmann, Coord. Chem. Rev. 206–207 (2000) 321.

[28] R. Duacheteau, Chem. Rev. 102 (2002) 3525.

[29] C. Copéret, M. Chabanas, R.P. Saint-Arroman, J.M. Basset, Angew. Chem. 115 (2003) 164;
C. Copéret, M. Chabanas, R.P. Saint-Arroman, J.M. Basset, Angew. Chem. Int. Ed. 42 (2003) 156.

[30] R.W.J.M. Hanssen, R.A. van Santen, H.C.L. Abbenhuis, Eur. J. Inorg. Chem. (2004) 675.

[31] K. Wada, D. Izuhara, M. Shiotsuki, T. Kondo, T. Mitsudo, Chem. Lett. (2001) 734.

[32] G. Hornyak, M. Kroll, R. Pugin, T. Sawitowsk, G. Schmid, J.O. Bovin, G. Karsson, H. Hofmeister, S. Hopfe, Chem. Eur. J. 3 (1997) 1951.

[33] G. Schmid, R. Pugin, J. Malm, J. Bovin, Eur. J. Inorg. Chem. (1998) 813.

[34] K. Naka, H. Itoh, Y. Chujo, Nano Lett. 2 (2002) 1183.

[35] X. Wang, K. Naka, H. Itoh, Y. Chujo, Chem. Lett. 33 (2004) 216.

[36] K. Naka, H. Itoh, Y. Chujo, Bull. Chem. Soc. Jpn. 77 (2004) 1767.

[37] K. Wada, M. Nakashita, A. Yamamoto, H. Wada, T. Mitsudo, Chem. Commun. (1998) 133.

[38] K. Wada, M. Nakashita, M. Bundo, K. Ito, T. Kondo, T. Mitsudo, Chem. Lett. (1998) 659.

[39] K. Wada, K. Yamada, T. Kondo, T. Mitsudo, Chem. Lett. (2001) 12.

[40] K. Wada, K. Yamada, T. Kondo, T. Mitsudo, J. Jpn. Pet. Inst. 45 (2002) 15.

[41] K. Wada, K. Tada, N. Itayama, T. Kondo, T. Mitsudo, J. Catal. 228 (2004) 374.

[42] N. Maxim, H.C.L. Abbenhuis, P.J. Stobbelaar, B.L. Mojet, R.A. van Santen, Phys. Chem. Chem. Phys. 1 (1999) 4473.

[43] N. Maxim, H.C.L. Abbenhuis, P.C.M.M. Magusin, R.A. van Santen, Chin. J. Chem. 19 (2001) 30.

[44] N. Maxim, P.C.M.M. Magusin, P.J. Kooyman, J.H.M.C. van Wolput, R.A. van Santen, H.C.L. Abbenhuis, Chem. Mater. 13 (2001) 2958.

[45] N. Maxim, A. Overweg, P.J. Kooyman, A. Nagy, R.A. van Santen, H.C.L. Abbenhuis, J. Mater. Chem. 12 (2002) 3792.

[46] N. Maxim, A. Overweg, P.J. Kooyman, J.H.M.C. van Wolput, R.W.J.M. Hanssen, R.A. van Santen, H.C.L. Abbenhuis, J. Phys. Chem. B 106 (2002) 2203.

[47] R. Murugavel, P. Davis, V. Shete, Inorg. Chem. 42 (2003) 4696.

[48] D.D. Perrin, W.L.F. Armarego, Purification of Laboratory Chemicals, third ed., Pergamon, Oxford, UK, 1988.

[49] K. Wada, K. Yano, T. Kondo, T. Mitsudo, submitted for publication.

[50] F. Moulder, W.F. Stickle, P.E. Sobol, K.D. Bomben, Handbook of X-ray Photoelectron Spectroscopy, Perkin-Elmer Co., Eden Prairie, USA, 1992.

[51] T. Iwasawa, M. Tokunaga, Y. Obora, Y. Tsuji, J. Am. Chem. Soc. 126 (2004) 6554.

[52] S.J. Greg, K.S.W. Sing, Adsorption, Surface Area and Porosity, second ed., Academic Press, London, UK, 1982.

[53] A. Saito, H.C. Foley, AIChE J. 37 (1991) 429.

[54] S. Iwamoto, W. Tanakulrungsank, K. Kagawa, P. Praserthdam, Ceram. Trans. 115 (2000) 643.

[55] J.E. Swain, M.V. Juskelis, J.P. Slanga, J.G. Miller, M. Uberoi, N.D. Spencer, Appl. Catal. A: Gen. 139 (1996) 175.

[56] A.I. Biaglow, R.J. Gorte, S. Srinvasan, A.K. Datye, Catal. Lett. 13 (1992) 313.